Interference between ϕ and $\Lambda(1520)$ production channels in $\gamma p \to K^+K^-p$ reaction near Threshold

Sun Young Ryu (RCNP, Osaka University)
for the LEPS Collaboration

Outline

1. Photoproduction of ϕ and $\Lambda(1520)$ near threshold.
2. Interference effect between ϕ and $\Lambda(1520)$ production channels.
3. Relative phase measurement.

Published in *Phys. Rev. Lett.* **116**, *232001 (2016)*

ϕ Meson Photoproduction

The ϕ-meson production has the unique feature within gluon dynamics of being a result of OZI suppression due to the dominant $\bar{s}s$ structure .

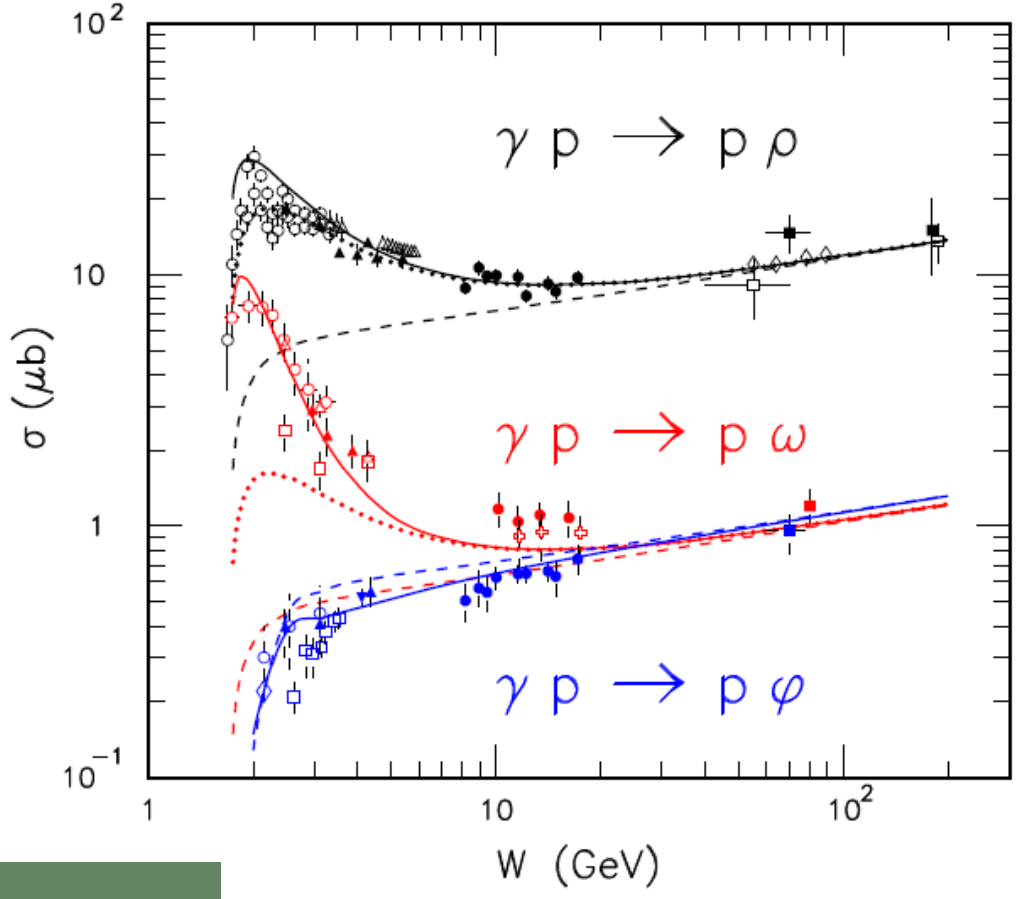

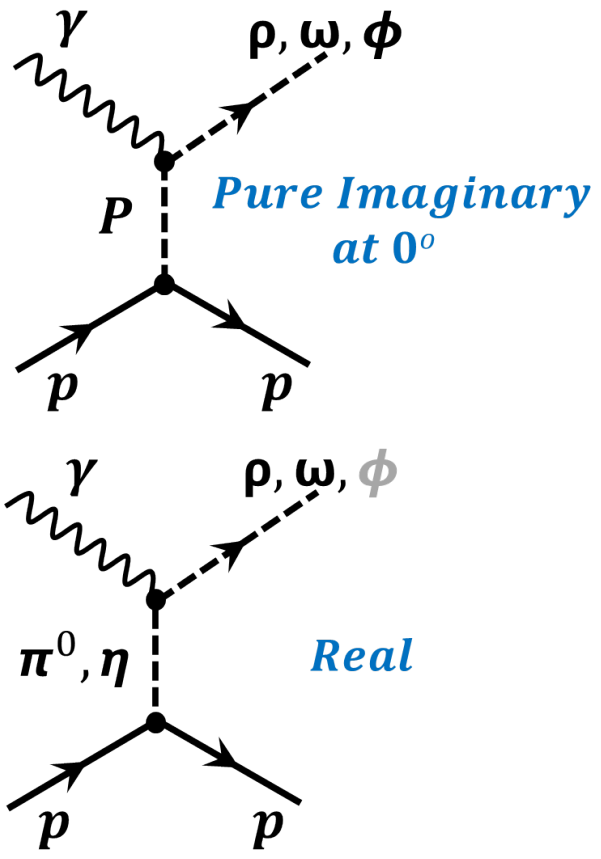

Bumps in ϕ Meson Photoproduction

- The $\sqrt{s} = 2.1$ GeV bump in ϕ photoproduction has not yet been explained in detail [1].

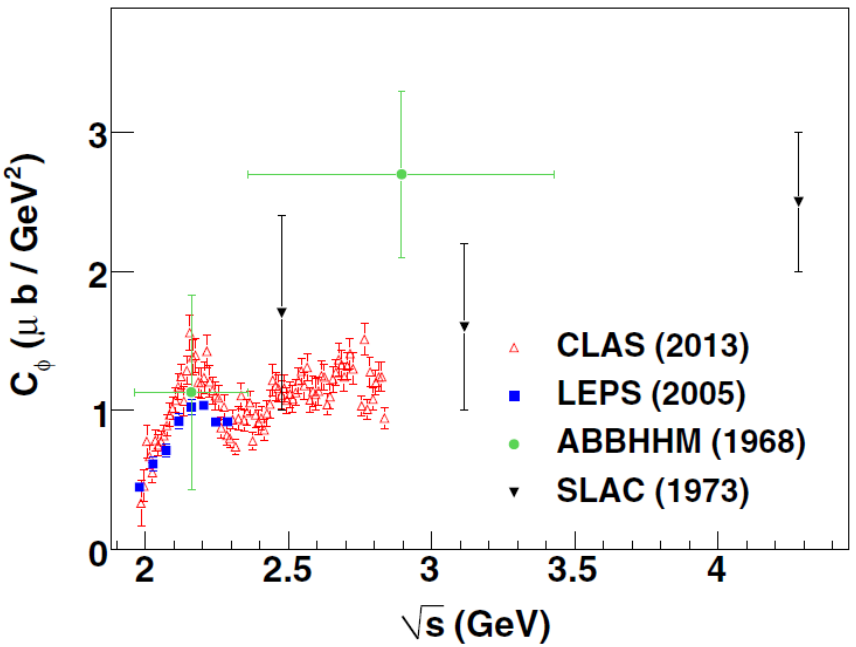

- ✓ Excitation of missing nucleon resonances [2]
- ✓ Hidden-strangeness pentaquark state [3]
- ✓ Rescattering processes [4]
- ✓ Interference effect between ϕ and $\Lambda(1520)$ production channels

[1] T. Mibe *et al.* (LEPS), PRL 95, 182001 (2005); H. Seraydaryan *et al.* (CLAS) PRC 89, 182001 (2005); B. Dey *et al.* (CLAS) PRC 89, 055206 (2014)
[2] A. Kiswandhi *et al.*, PLB 691, 214 (2010)
[3] R. Aaji *et al.* (LHCb), PRL 115, 072001 (2015)
[4] S. Ozaki *et al.*, PRC 80, 035201 (2009); H-Y. Ryu *et al.*, PTEP 2014, 023D03 (2014)

Bumps in ϕ and $\Lambda(1520)$ Photoproduction

- Similar bump in $\Lambda(1520)$ photoproduction [5] .

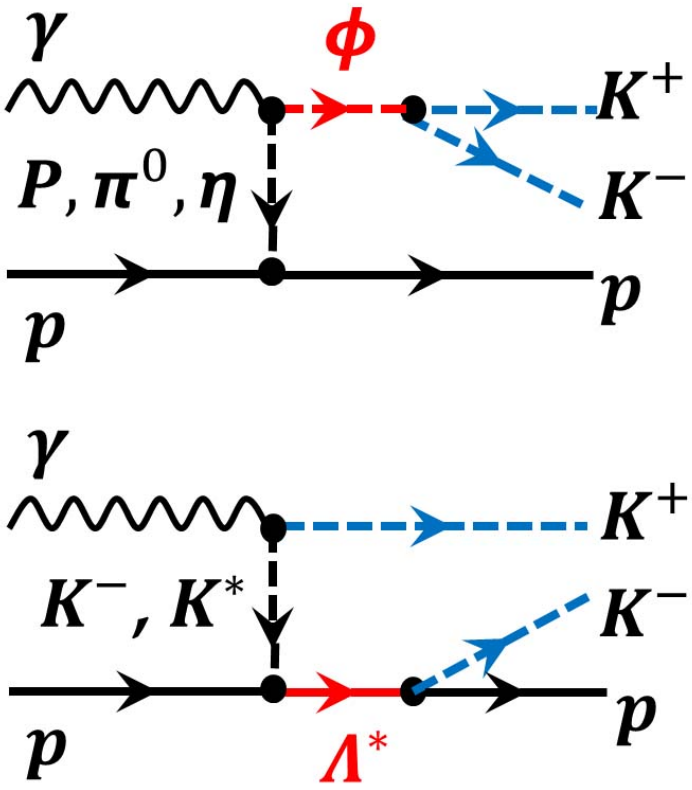

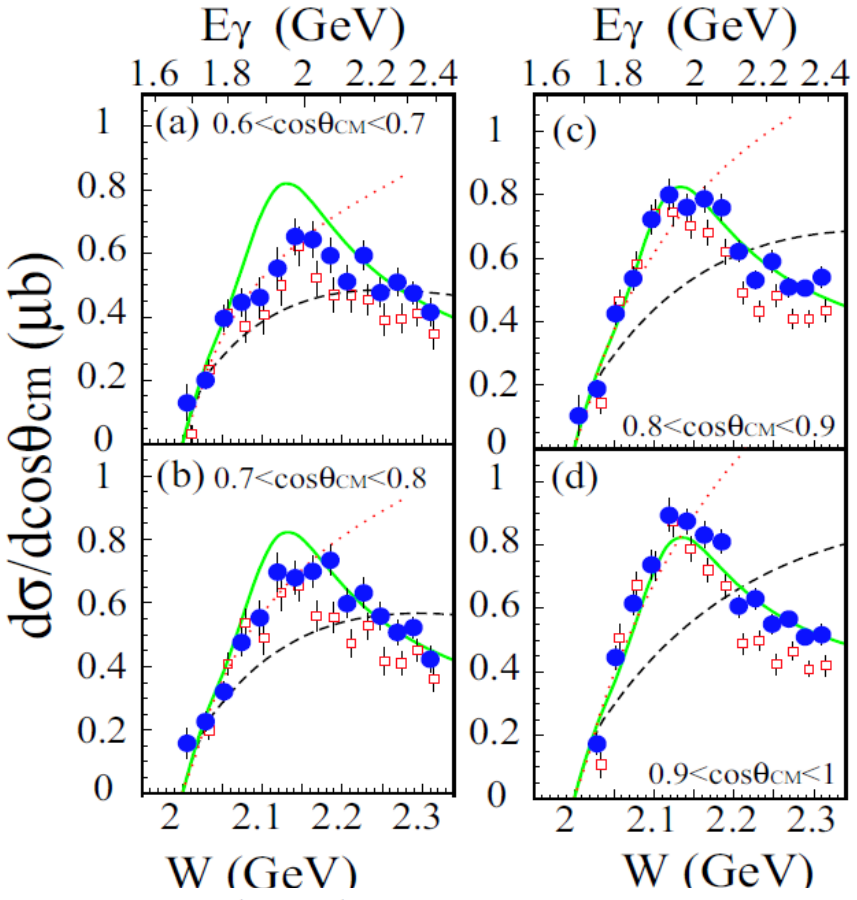

[5] H. Kohri *et al.* (LEPS), PRL 108, 092001 (2012)

Differential Cross Sections for $\gamma\ p \to K^+K^-p$

$$\frac{\mathrm{d}^2\sigma}{\mathrm{d}m_{K^+K^-}\mathrm{d}m_{K^-p}} \propto |\mathcal{M}_{\phi} + \mathcal{M}_{\Lambda(1520)} + \mathcal{M}_{\mathrm{nr}}|^2$$

$$\approx |\mathcal{M}_{\phi} + \mathcal{M}_{\Lambda(1520)}|^2 + |\mathcal{M}_{\mathrm{nr}}|^2,$$

where $\mathcal{M}_{\phi}$ and $\mathcal{M}_{\Lambda(1520)}$ are the complex amplitudes for ϕ and $\Lambda(1520)$ production processes, respectively. $\mathcal{M}_{nr}$ represents non-resonant K^+K^-p production.

Interference between $\phi(1020)$ and $\Lambda(1520)$

Differential cross sections for the $\gamma p \to K^+K^-p$ reaction via the ϕ and $\Lambda(1520)$ resonances:

$$\left.\frac{\mathrm{d}^2\sigma}{\mathrm{d}m_{K^+K^-}\mathrm{d}m_{K^-p}}\right|_{\phi,\Lambda(1520)}$$

$$\propto \left| \underbrace{\frac{a\, e^{i\psi_a}}{m_\phi^2 - m_{K^+K^-}^2 + i m_\phi \Gamma_\phi}}_{\mathcal{M}_\phi} + \underbrace{\frac{b\, e^{i\psi_b}}{m_{\Lambda^*}^2 - m_{K^-p}^2 + i m_{\Lambda^*} \Gamma_{\Lambda^*}}}_{\mathcal{M}_{\Lambda(1520)}} \right|^2,$$

where $a = a(E_\gamma)$ and $b = b(E_\gamma)$ denote the magnitudes of the Breit-Wigner amplitudes for ϕ and $\Lambda(1520)$.

Interference between $\mathcal{M}_{\phi}$ and $\mathcal{M}_{\Lambda(1520)}$

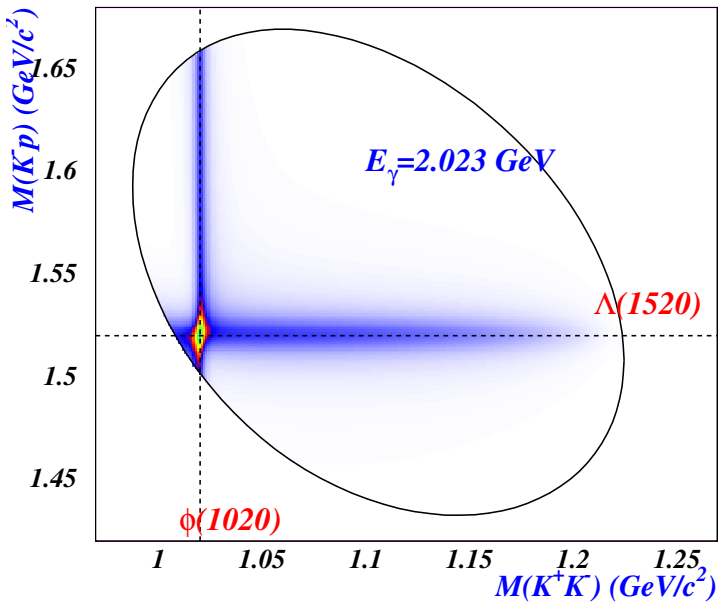

The integrated cross sections over the $K^- p$ mass interval in the ϕ-$\Lambda(1520)$ interference region where the two resonances overlap [6]:

$$B(m_{K^+K^-}) = B(m_{K^+K^-}, E_\gamma)$$

Theoretical calculation [7]

$$\frac{d\sigma}{dm_{K^+K^-}} \propto \left| \frac{a e^{i\psi_a}}{m_\phi^2 - m_{K^+K^-}^2 + i m_\phi \Gamma_\phi} + B(m_{K^+K^-}) e^{i\psi_b} \right|^2$$

[6] Y. Azimov, J. Phys. G 37, 023001(2010)
[7] S. i. Nam et al. (to be published) for the theoretical calculation approach

Interference between $\mathcal{M}_\phi$ and $\mathcal{M}_{\Lambda(1520)}$

where $\psi = |\psi_a - \psi_b|$ is the relative phase between a and B, $m = m_{K^+K^-}$.

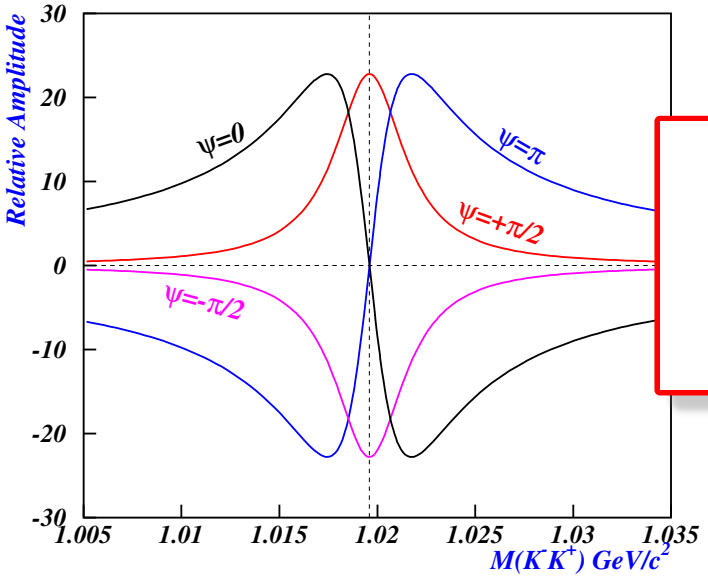

$$\frac{|a|^2}{(m_\phi^2 - m^2)^2 + m_\phi^2\Gamma_\phi^2} + |B(m)|^2 +$$

$$\frac{2(m_\phi^2 - m^2)|aB|\cos\psi + 2\Gamma_\phi m_\phi |aB|\sin\psi}{(m_\phi^2 - m^2)^2 + m_\phi^2\Gamma_\phi^2}$$

Maximum constructive at $\psi = +\pi/2$

Maximum destructive at $\psi = -\pi/2$.

Interference Analysis

- Event selection with kinematic fits for $\gamma p \to K^+ K^- p$.

Interference Analysis

- Event selection with kinematic fits for $\gamma p \rightarrow K^+K^-p$.
- Determinations of $|\mathcal{M}_{\phi}|^2 : a$ and $|\mathcal{M}_{\Lambda(1520)}|^2 : B(m_{K^+K^-})$ by excluding the possible interference region* with the $0.1\ GeV$ energy interval.

Interference Analysis

- Event selection with kinematic fits for $\gamma p \rightarrow K^+K^-p$.
- Determinations of $|\mathcal{M}_\phi|^2 : a$ and $|\mathcal{M}_{\Lambda(1520)}|^2 : B(m_{K^+K^-})$ by excluding the possible interference region* with the $0.1\ GeV$ energy interval.

  * $|M_{K^+K^-} - m_\phi| < 4\ \Gamma_\phi, \qquad \Gamma_\phi = 4.266$ MeV

Interference Analysis

- Event selection with kinematic fits for $\gamma p \rightarrow K^+K^-p$.
- Determinations of $|\mathcal{M}_{\phi}|^2 : a$ and $|\mathcal{M}_{\Lambda(1520)}|^2 : B(m_{K^+K^-})$ by excluding the possible interference region* with the $0.1\ GeV$ energy interval.

  * $|M_{K^+K^-} - m_{\phi}| < 4\ \Gamma_{\phi}, \qquad \Gamma_{\phi} = 4.266$ MeV

  * $|\ M_{K^-p} - m_{\Lambda^*}\ | < 2\ \Gamma_{\Lambda^*}, \qquad \Gamma_{\Lambda^*} = 15.6$ MeV

Interference Analysis

- Event selection with kinematic fits for $\gamma p \rightarrow K^+K^-p$.
- Determinations of $|\mathcal{M}_\phi|^2 : a$ and $|\mathcal{M}_{\Lambda(1520)}|^2 : B(m_{K^+K^-})$ by excluding the possible interference region* with the $0.1\ GeV$ energy interval.
  - * $|M_{K^+K^-} - m_\phi| < 4\,\Gamma_\phi, \qquad \Gamma_\phi = 4.266$ MeV
  - * $|\,M_{K^-p} - m_{\Lambda^*}\,| < 2\,\Gamma_{\Lambda^*}, \qquad \Gamma_{\Lambda^*} = 15.6$ MeV
- Relative phase measurement between ϕ and $\Lambda(1520)$ amplitudes in terms of energy in the interference region*.

Interference Analysis

- Event selection with kinematic fits for $\gamma p \rightarrow K^+K^-p$.
- Determinations of $|\mathcal{M}_{\phi}|^2 : a$ and $|\mathcal{M}_{\Lambda(1520)}|^2 : B(m_{K^+K^-})$ by excluding the possible interference region* with the $0.1\ GeV$ energy interval.
  - * $|M_{K^+K^-} - m_{\phi}| < 4\ \Gamma_{\phi}, \qquad \Gamma_{\phi} = 4.266$ MeV
  - * $|\ M_{K^-p} - m_{\Lambda^*}\ | < 2\ \Gamma_{\Lambda^*}, \qquad \Gamma_{\Lambda^*} = 15.6$ MeV
- Relative phase measurement between ϕ and $\Lambda(1520)$ amplitudes in terms of energy in the interference region*.
- Measurement of Cross sections for ϕ and $\Lambda(1520)$ photoproduction by excluding the possible interference region*.

Experiment at LEPS/SPring-8

- Compton-Backscattered photon beam and a forward LEPS spectrometer at BL33LEP beam line, SPring-8.
- $\gamma p \to K^- K^+ p$ reactions at forward angles from the ϕ production threshold (1.573 GeV) to 2.4 GeV.

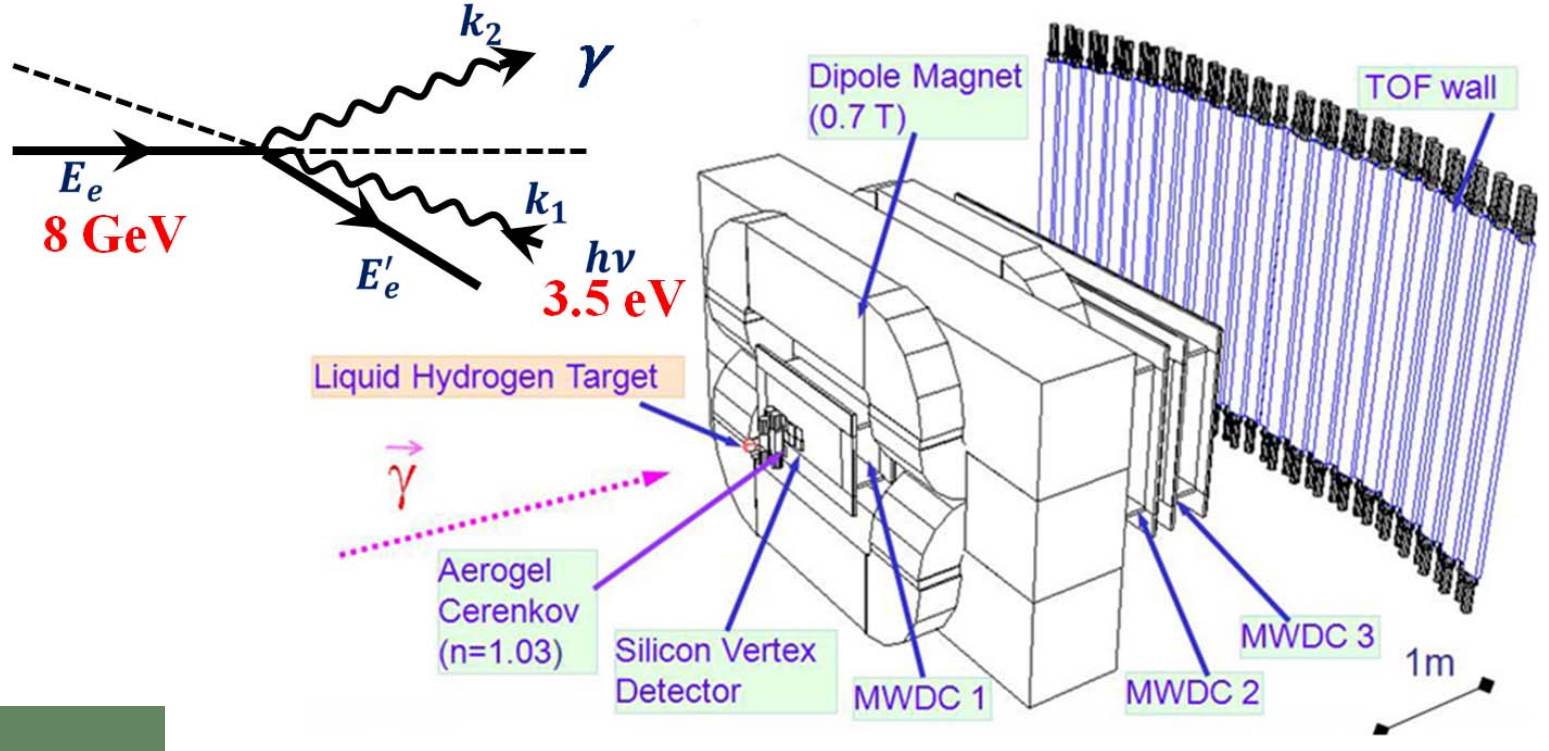

Particle Identification

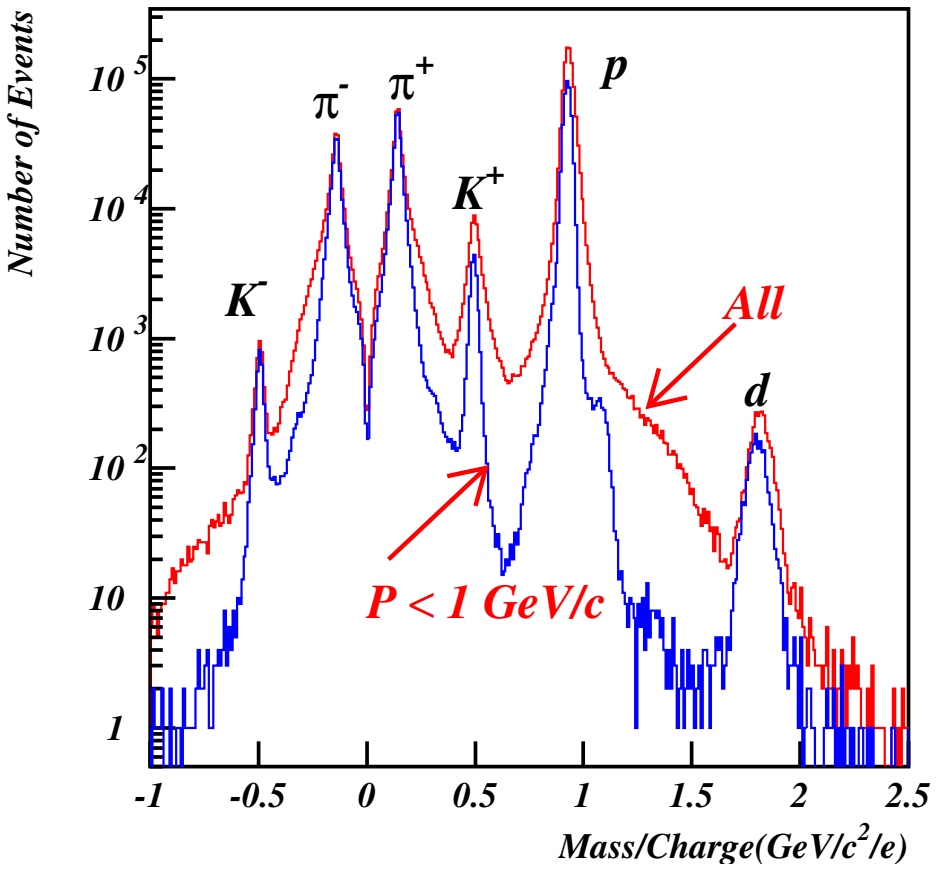

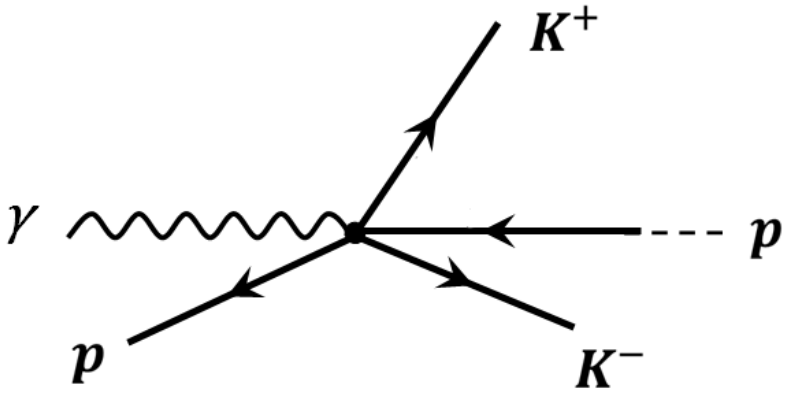

K^+K^- Detection

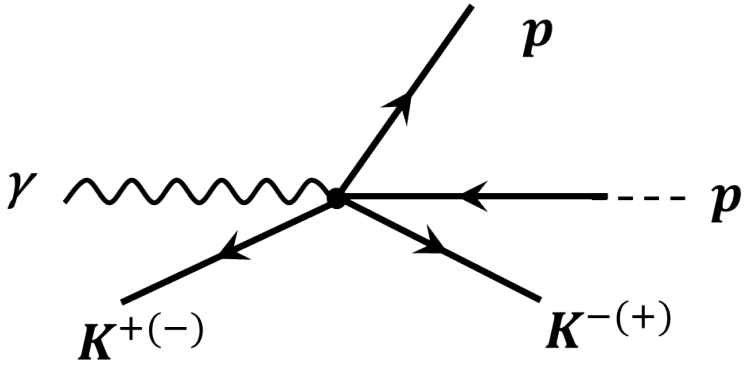

$K^-(K^+)p$ Detection

- A typical mass resolution is 30 MeV for 1 GeV kaons.

K^+K^-p Events from Kinematic Fit $P(\chi^2) > 0.02$

K^+K^- detection

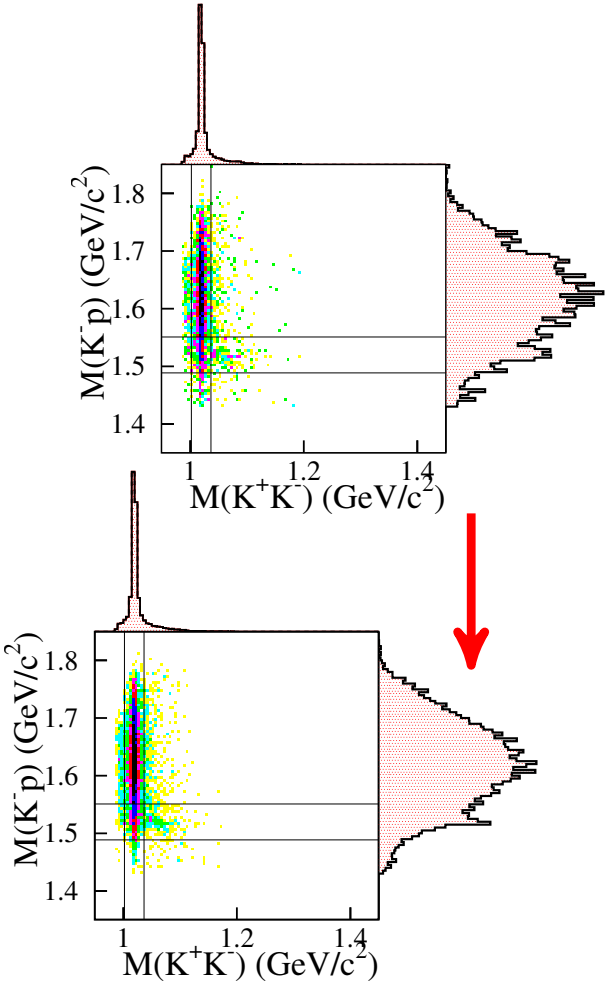

K^-p detection

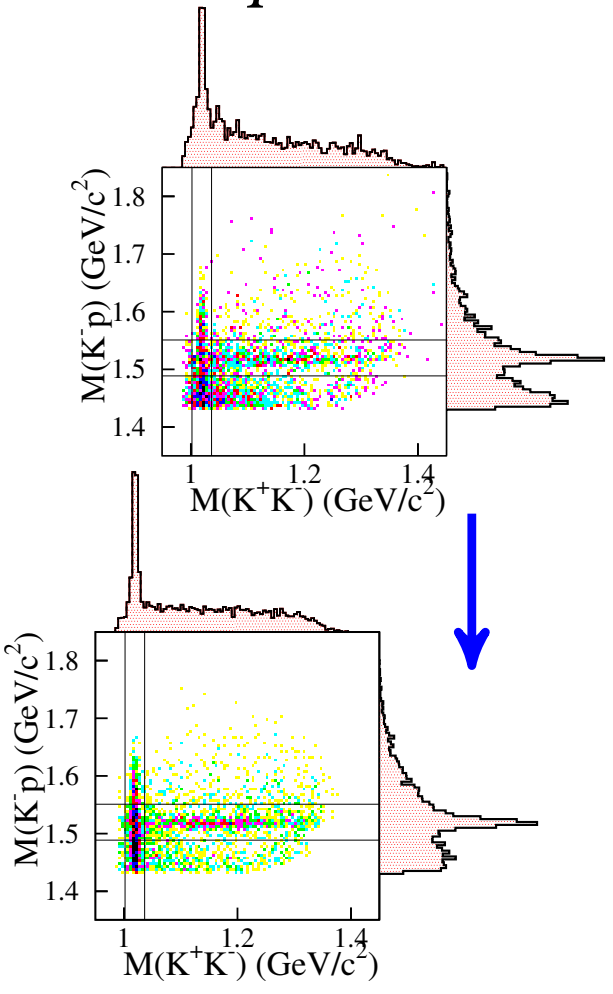

K^+p detection

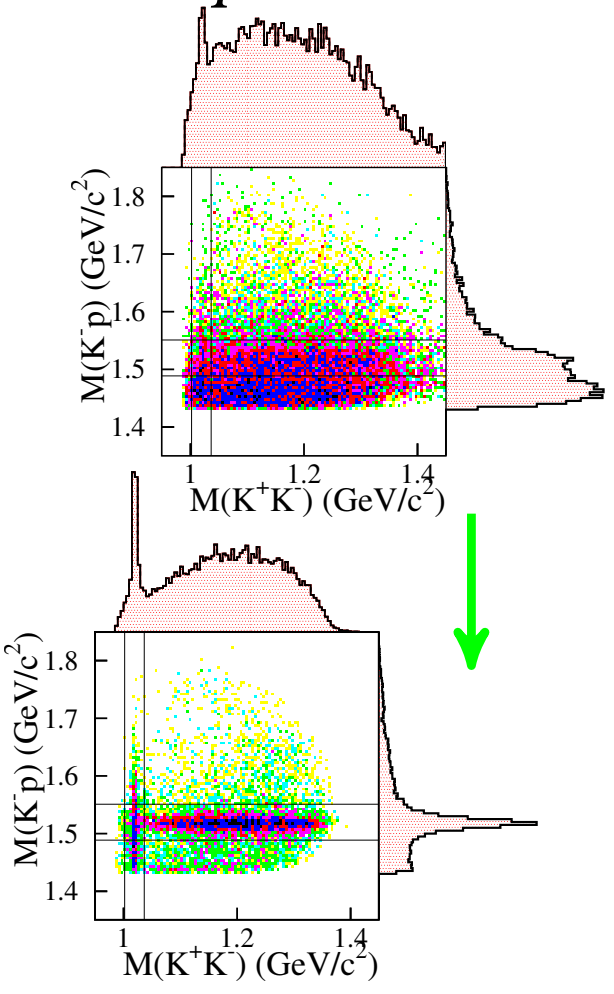

MC Simulation for $\gamma p \to K^+K^-p$ in all E_γ Ranges

MC ϕ MC Λ^* MC Swave MC $K^*(896)$

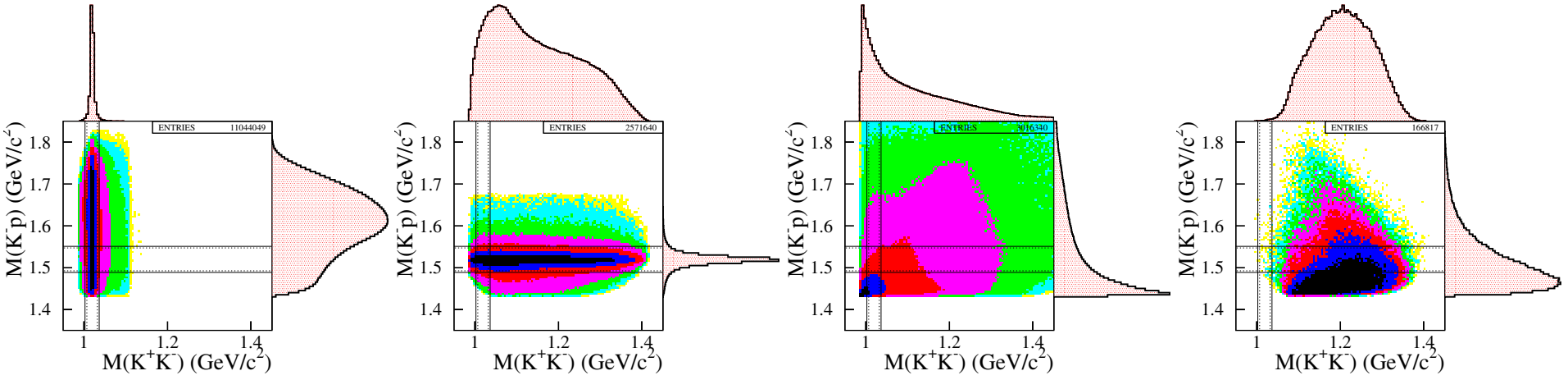

1. $\gamma p \to \phi p \to K^-K^+p$ based on E_γ-dependent SDME [2].
2. $\gamma p \to \Lambda(1520)K^+ \to K^-pK^+$ based on the decay angular distributions from LEPS results [3].
3. $\gamma p \to K^+K^-p$ (non-resonant S-wave production)
4. $\gamma p \to K(896)^0\Sigma^+ \to K^+\pi^-p\pi^0$ based on SDME results [4].

[2] W.C. Chang *et al.* (LEPS) PRC 82, 015205 (2010)
[3] J. Chen, Ph.D thesis (2009)
[4] S.H. Hwang *et al.* (LEPS), PRL 108, 092001 (2012)

2-D Fits except the Interference Region

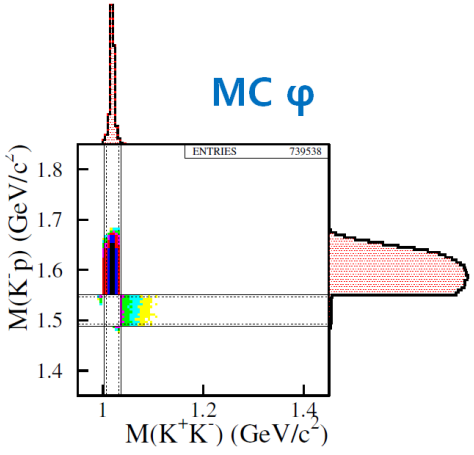

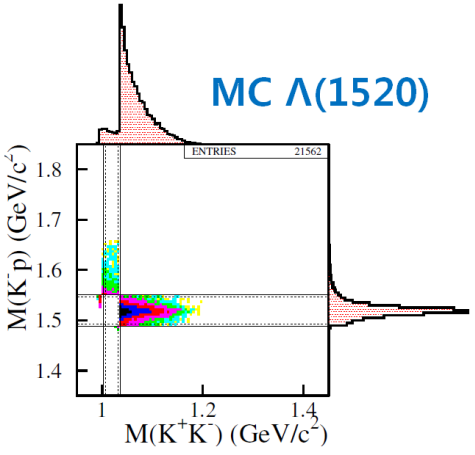

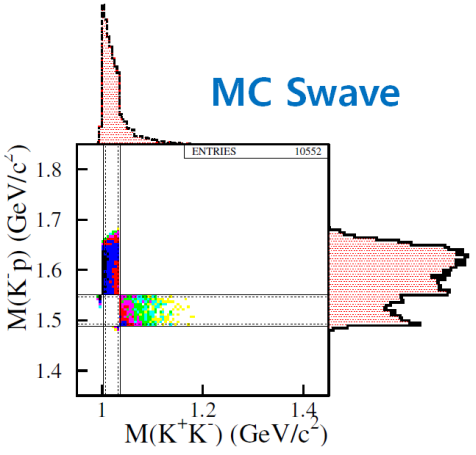

- $|\mathcal{M}_\phi|^2$ and $|\mathcal{M}_{\Lambda(1520)}|^2$ in the interference region are estimated from the magnitudes of MC templates for ϕ and $\Lambda(1520)$ mass bands.

2-D Fit with MC Templates for $\gamma p \to K^- K^+ (p)$

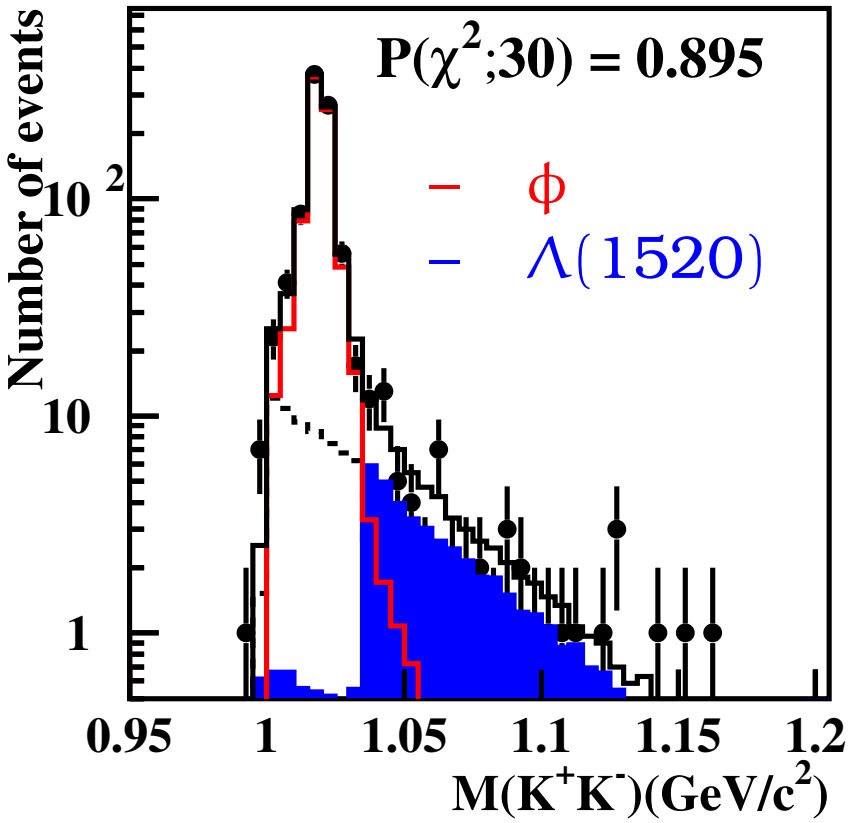

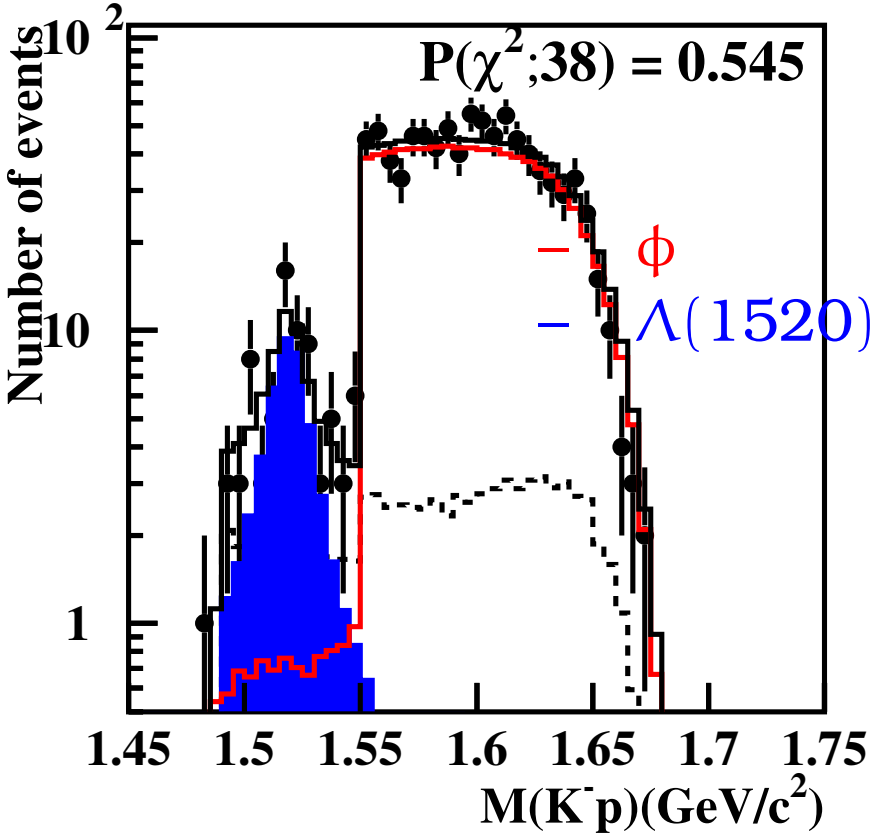

- : The invariant mass spectra for K^+K^-(left) and K^-p(right) system

----- : MC data for non-resonant K^+K^-p production

Interference Region $K^+K^-(p)$

Utilizing the MC linshapes in Interference Region

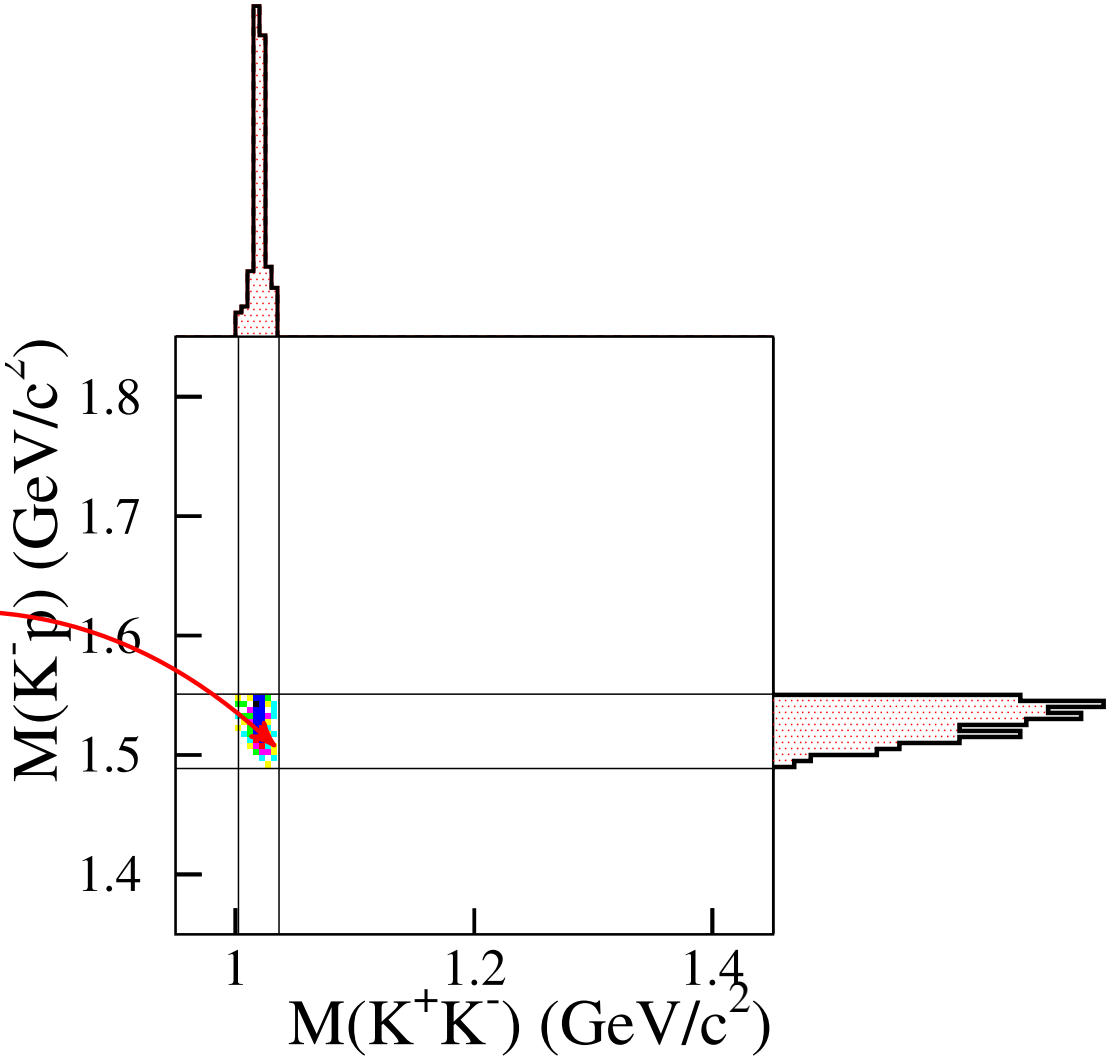

Interference Yields (K^+K^-)

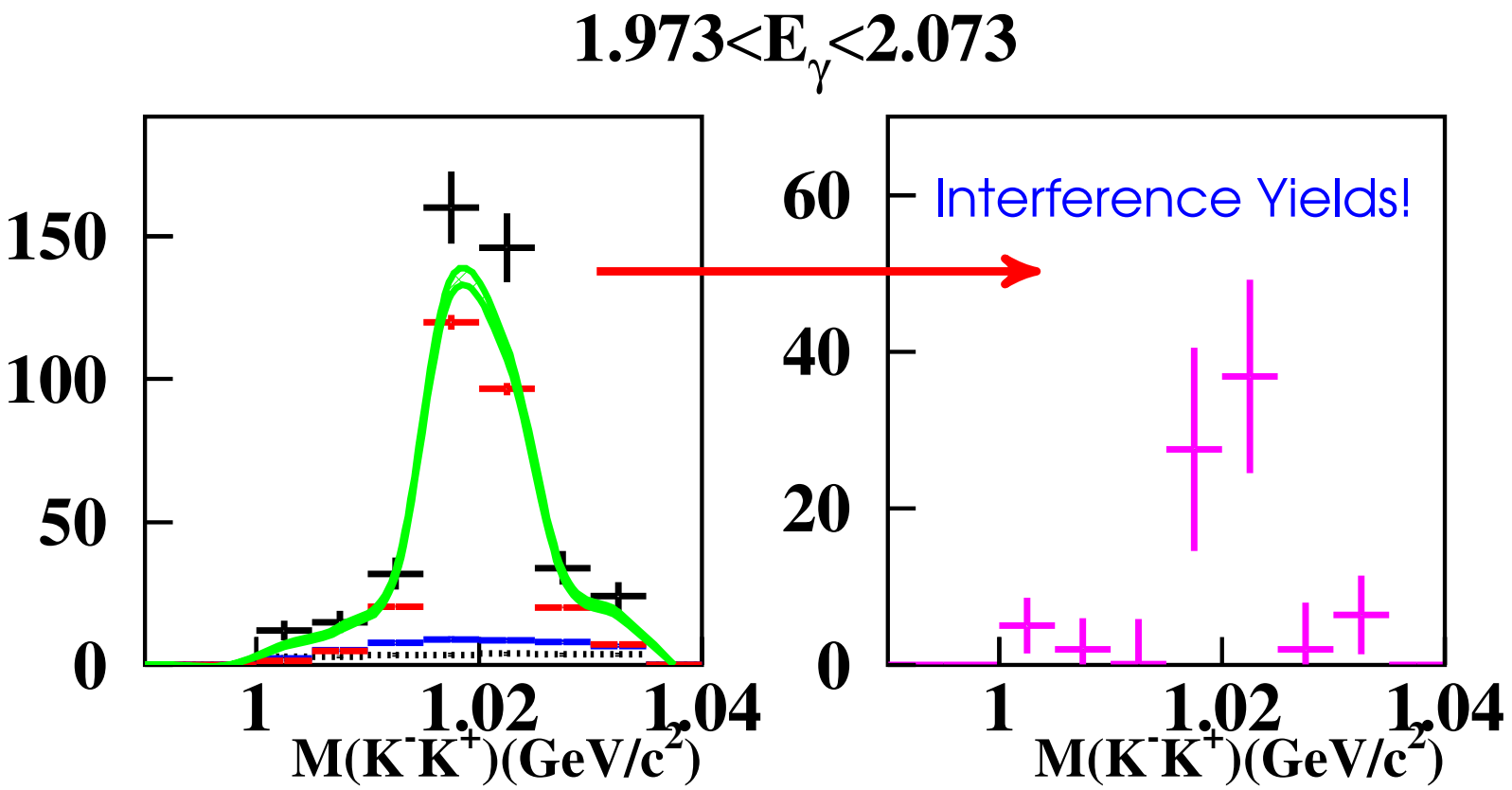

+ : $|\mathcal{M}_\phi + \mathcal{M}_{\Lambda(1520)}|^2 + |\mathcal{M}_{\rm nr}|^2$, **−** : $|\mathcal{M}_\phi|^2 + |\mathcal{M}_{\Lambda(1520)}|^2 + |\mathcal{M}_{\rm nr}|^2$

Fit results for the relative phase (K^+K^-)

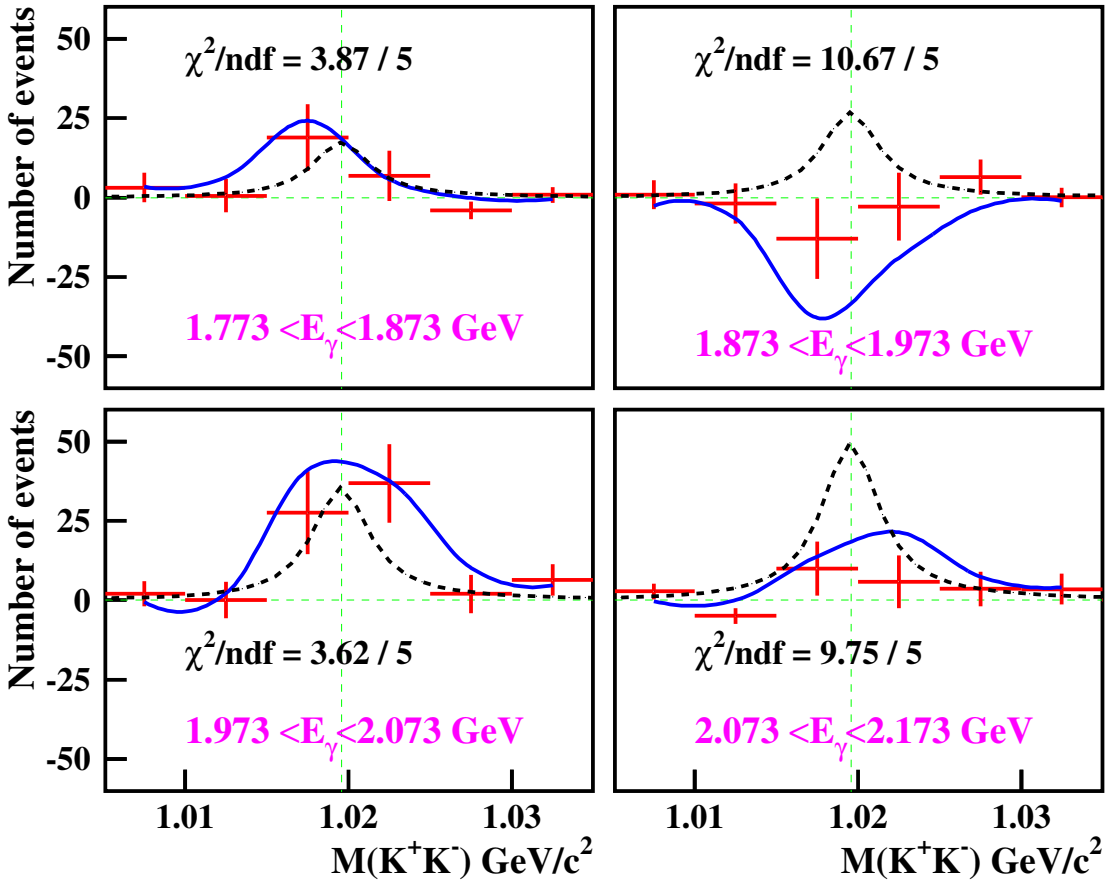

ψ	$P(\chi^2, 5; \psi)$
$69^o \pm 13^o$	56.8%
$-86^o \pm 9^o$	5.8%
$98^o \pm 7^o$	60.5%
$141^o \pm 10^o$	8.3%

Dashed lines are from theoretical estimates with $\psi = \pi/2$ (S. i. Nam *et al.*)

Integrated Yields and Phases (K^+K^-)

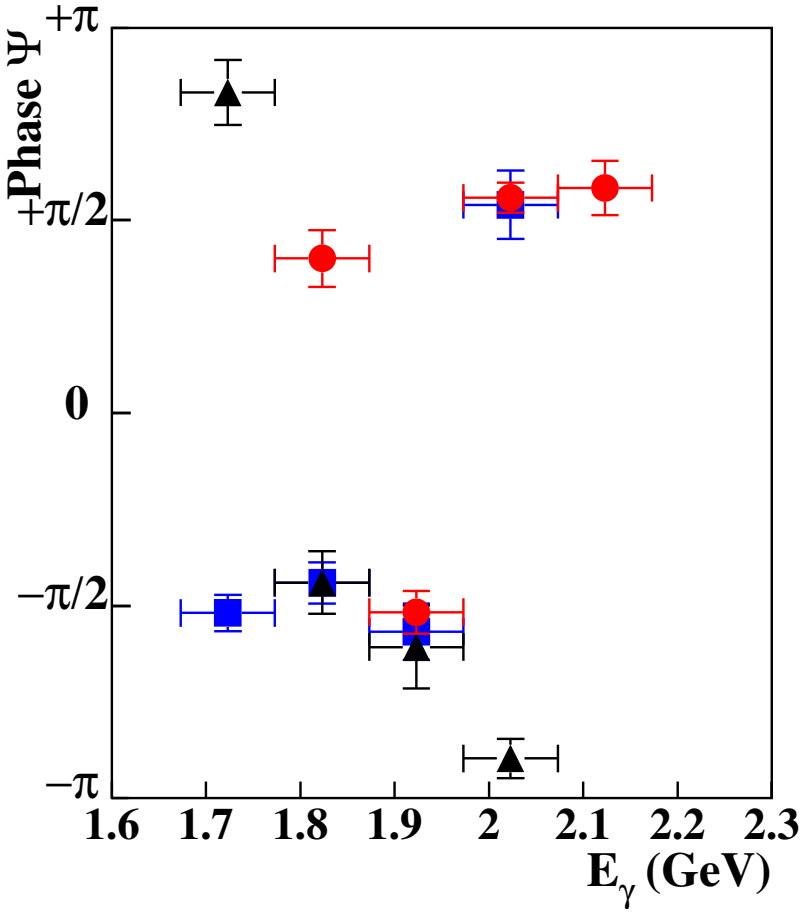

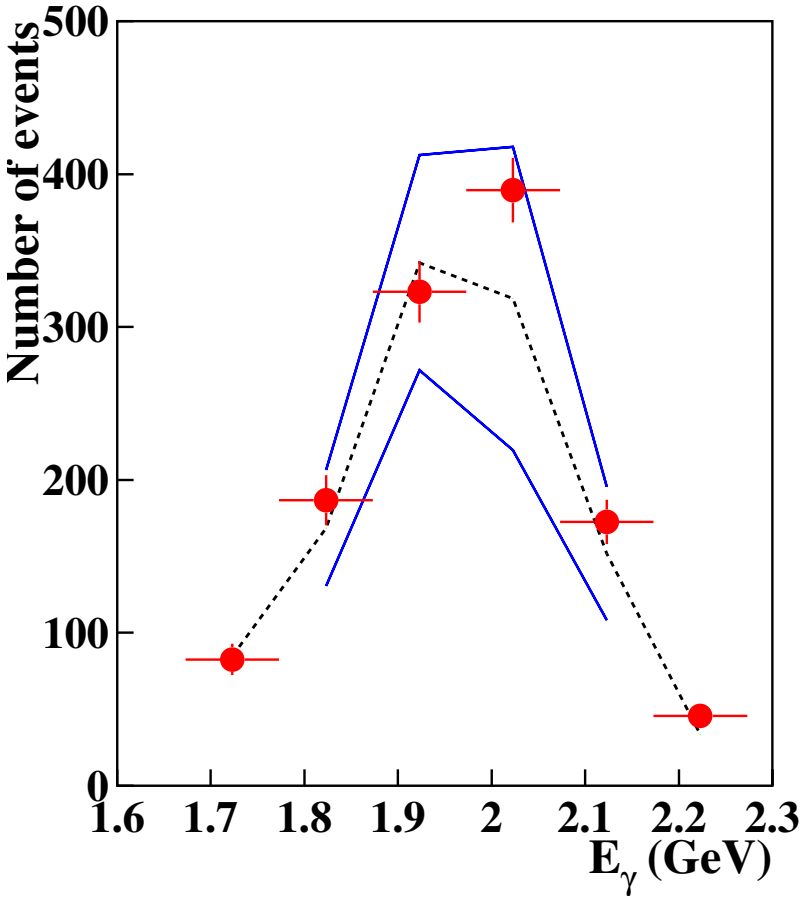

● K^+K^- mode ■ K^-p mode ▲ K^+p mode

Forward Differential Cross section for $\gamma p \to \phi p$

- We reconfirm the bump structure at $\sqrt{s} = 2.1$ GeV.

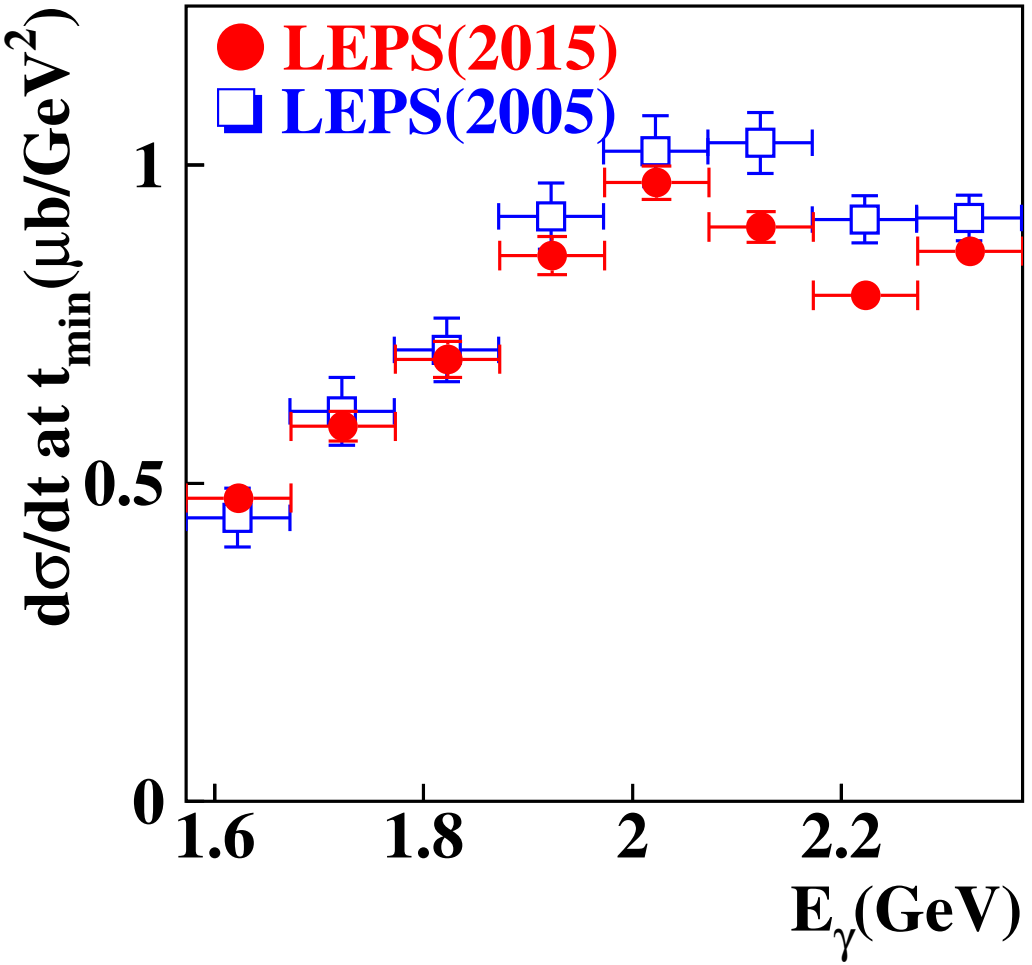

Differential Cross Sections for $\gamma p \to K^+\Lambda(1520)$

- We also reconfirm the bump structure for $\gamma p \to K^+\Lambda(1520)$ at forward angles.

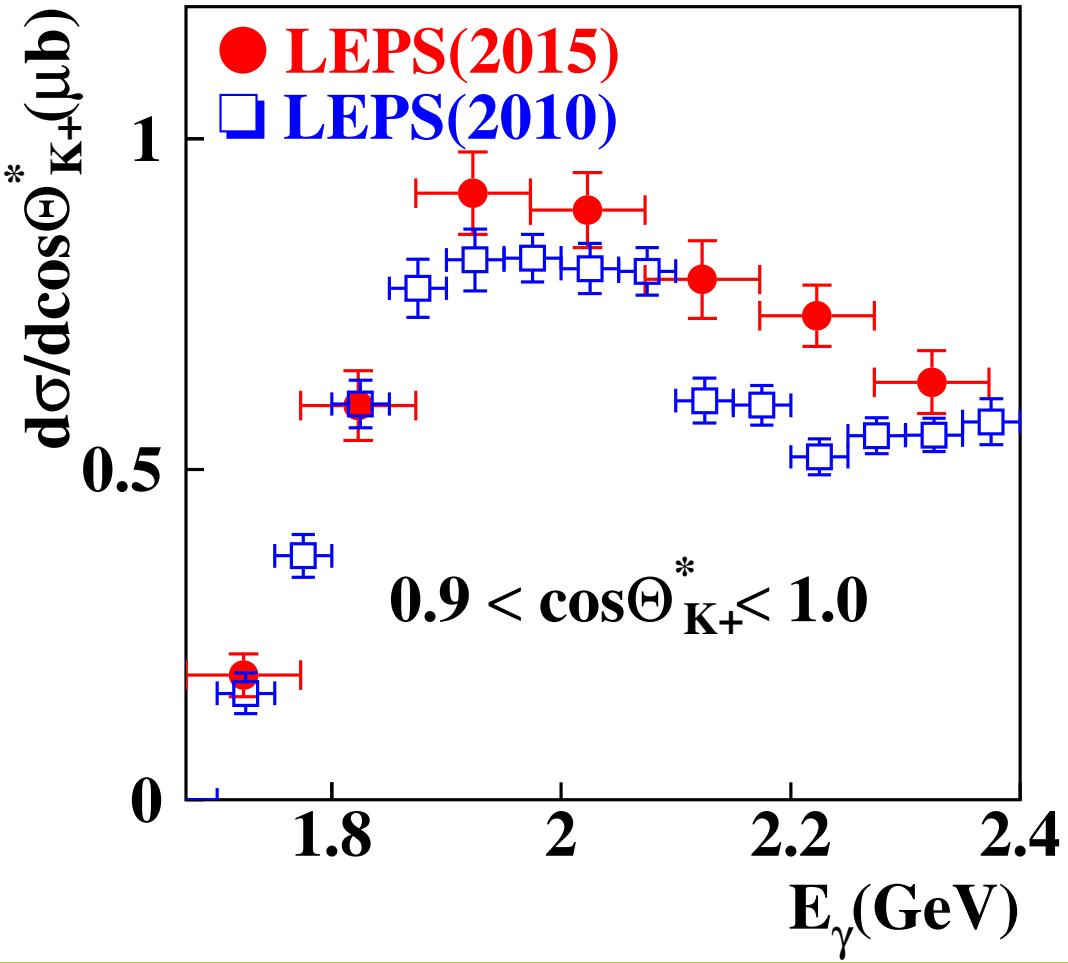

Summary

- The ϕ-$\Lambda(1520)$ interference measurement is a good probe to study the origin of enhanced production cross sections for ϕ and $\Lambda(1520)$ near $\sqrt{s}$=2.1GeV.

Summary

- The ϕ-$\Lambda(1520)$ interference measurement is a good probe to study the origin of enhanced production cross sections for ϕ and $\Lambda(1520)$ near $\sqrt{s}$=2.1GeV.
- The relative phases suggest strong constructive interference for K^+K^- pairs observed at forward angles.

Summary

- The ϕ-$\Lambda(1520)$ interference measurement is a good probe to study the origin of enhanced production cross sections for ϕ and $\Lambda(1520)$ near $\sqrt{s}$=2.1GeV.
- The relative phases suggest strong constructive interference for K^+K^- pairs observed at forward angles.
- We reconfirmed the bump structure and found that ϕ-$\Lambda(1520)$ interference effect is not large enough to account for the bump structure.

Summary

- The ϕ-$\Lambda(1520)$ interference measurement is a good probe to study the origin of enhanced production cross sections for ϕ and $\Lambda(1520)$ near $\sqrt{s}$=2.1GeV.
- The relative phases suggest strong constructive interference for K^+K^- pairs observed at forward angles.
- We reconfirmed the bump structure and found that ϕ-$\Lambda(1520)$ interference effect is not large enough to account for the bump structure.
- The nature of the bump structure could originate from interesting exotic structures such as a hidden-strangeness pentaquark state, a new Pomeron exchange or rescattering processes via other hyperon states.